

Supporting Online Material: Strong coupling between single electron tunneling and nano-mechanical motion

G. A. Steele¹, A. K. Hüttel^{1,*}, B. Witkamp¹, M. Poot¹, H. B. Meerwaldt¹, L. P. Kouwenhoven¹
and H. S. J. van der Zant¹

¹*Kavli Institute of NanoScience, Delft University of Technology, PO Box 5046, 2600 GA, Delft, The Netherlands.*

S1 Materials and Methods

S1.1 Device description

The fabrication is described detail in [1] and [2]: briefly, a trench in a silicon oxide layer is defined by dry etching, and W/Pt electrodes are deposited to act as source and drain contacts for injecting current. In device 1, the oxide is then further wet-etched by approximately 100 nm to ensure the nanotube is completely suspended. The nanotube is grown in the last step of the fabrication to ensure the nanotube is not damaged by electron beam irradiation or contaminated with residue from chemical processing.

The length of the trench in device 1 is 800 nm. The nanotube in device 1 has a large bandgap of \sim 300 mV, estimated from the gate voltage range of depletion of carriers seen in transport measurements, and a diameter of \sim 3 nm, determined from the orbital magnetic moment of the nanotube. The quantum dot displays a clean four fold shell filling pattern over a wide range of gate voltages corresponding to hundreds of Coulomb peaks. In device 1, we drive mechanical oscillations of the devices using an electric field from a nearby antenna consisting of an unterminated coaxial cable placed \sim 2 cm from the sample. The mechanical nature of the resonance is confirmed by tuning the nanotube tension using the gate [2, 3, 4].

In device 2, the dry etch is aligned to the source and contacts, and so a second wet etch is not required. The nanotube in device 2 has a bandgap of \sim 100 mV, determined from the size of the empty dot Coulomb diamond [1]. The trench in device 2 has a length of 430 nm. For device 2, we did not have a high frequency coax for exciting the mechanical resonance: however, we estimate the resonance frequency to be in the range of 100 to 500 MHz, based on the length of the suspended segment.

We have cooled down \sim 12 suspended nanotube devices made using this ultra-clean fabrication technique, with trenches ranging from 430 nm to 1100 nm. All of these devices displayed the switch-ridges in dI/dV discussed in Fig. 4 of the main text.

S1.2 Normalization of the resonance signal

As the shift ΔI of the d.c. current from the mechanical resonance is proportional to the curvature of the Coulomb peak [2], it changes in sign and significantly in magnitude at different gate voltages. In order to clearly show the position of the resonance in Fig. 2 and Fig. S1 at all gate voltages, we normalize the frequency sweep at each gate voltage by subtracting the average off-resonant current, taking the absolute value, and then normalizing to a range of 0 to 1.

S2 Supplementary Text

S2.1 Single electron tuning shifts of 0.5 MHz

In Fig. 2 of the main text, we showed offsets of the resonator frequency of 0.1 MHz due to the static charge of a single electron. The data from Fig. 2 of the text was taken around $V_g \sim -1$ V. In Fig. S1, we show the resonance frequency as a function of gate voltage around $V_g \sim -5$ V. Here, we observe offsets of the resonator frequency of 0.5 MHz. At larger gate voltages, the frequency tuning curve shown in Fig. 1C of the main text becomes steeper, and thus the offset in frequency from the single electron charge becomes larger. Although the nanotube quantum dot charge still increases by only one electron, this electron exerts a larger force on the nanotube due to its stronger attraction to the larger total charge on the gate.

*Present address: Institute for Experimental and Applied Physics, University of Regensburg, 93040 Regensburg, Germany

S2.2 Frequency softening by Coulomb blockade

The dips in the frequency of the mechanical oscillator, shown in Figs. 2 and 3 of the main text, arise from a softening of the electrostatic component of the spring constant of the mechanical motion due to Coulomb blockade [5]. To calculate this softening, we begin with the electrostatic force between the dot and the gate, given by

$$F_{dot} = \frac{1}{2} \frac{dC_g}{dz} (V_g - V_{dot})^2 \quad (\text{S1})$$

where C_g is the capacitance of the quantum dot to the gate, V_{dot} is the electrostatic potential of the quantum dot, and z is the vertical distance between the nanotube and the quantum dot. Since V_g is fixed and dC_g/dz is slowly varying, changes in this force will be dominated by changes in V_{dot} . The voltage on the dot is found from electrostatics:

$$V_{dot} = \frac{C_g V_g + q_{dot}}{C_{dot}} \quad (\text{S2})$$

where C_{dot} is the total capacitance of the quantum dot, and q_{dot} is the charge on the quantum dot. In Coulomb blockade, the charge on the dot does not increase continuously with gate voltage, but instead increase in discrete steps of one electron, as illustrated in Fig. S2A. As a result, the electrostatic potential on the dot will oscillate in a sawtooth pattern with an amplitude of e/C_{dot} , as shown in Fig. S2A. We write the charge on the dot as:

$$q_{dot} = -|e|N(q_c) \quad (\text{S3})$$

where N is the average number of electrons on the quantum dot, and $q_c = C_g V_g$ is the “control charge”. Note that the control charge is not the charge on the gate: the charge on the gate is given by the voltage difference from the gate to the dot, $q_g = C_g(V_g - V_{dot})$. The control charge is a concept we use here to express the idea that the quantum dot is controlled by both the voltage on the gate V_g and by the (distance dependent) capacitance to the gate $C_g(z)$. The control charge is the continuous charge that would be on the quantum dot in the absence of Coulomb blockade ($V_{dot} = 0$).

In the ideal limit of zero temperature and opaque tunnel barriers, N would follow a staircase with sharp steps (Fig. S2A solid line), and the sawtooth oscillation of V_{dot} would have sharp edges (Fig. S2B solid line). In practice, however, the electron number near the transition will fluctuate in time due to finite temperature and tunnel coupling to the leads. The transitions in the average charge $\langle N \rangle$ are then smooth, acquiring a finite width (dashed lines in Fig. S2A and B). The timescale of these fluctuations is set by the tunneling time Γ^{-1} . If the mechanical motion is much slower than Γ , the resonator will feel a force averaged over these fluctuations, which can be calculated using the time averaged expression for $\langle N(q_c) \rangle$. To find correction to the mechanical spring constant Δk from this force, we take the derivative of Eq. S1 with respect to the displacement of the nanotube:

$$\Delta k = -\frac{dF_{dot}}{dz} = (V_g - V_{dot}) \frac{dC}{dz} \frac{dV_{dot}}{dz} \quad (\text{S4})$$

(neglecting slowly varying terms d^2C_g/dz^2). Using Eq. S2 and S3, we obtain:

$$\Delta k = \frac{V_g(V_g - V_{dot})}{C_{dot}} \left(\frac{dC_g}{dz} \right)^2 \left(1 - |e| \frac{d\langle N \rangle}{dq_c} \right) \quad (\text{S5})$$

Note that the second term in the brackets on the right leads to a softening of the spring constant of the resonator, proportional to how quickly the average quantum dot occupation changes through a charge transition (i.e. the Coulomb peak). The strong peak in $d\langle N \rangle/dq_c$ at the steps of the Coulomb staircase leads to the large dips in the resonance frequency we observe in Figs. 2 and 3 in the main text. The softening that arises from the negative sign in front of $d\langle N \rangle/dq_c$ in Eq. S5 is very non-intuitive: we expect that increasing the charge on the nanotube will, in general, pull the nanotube towards the gate, increasing the tension and stiffening the spring constant. Here, increasing the charge instead *softens* the spring constant.

Physically, this softening comes from the peculiar screening properties of a Coulomb blockaded quantum dot, illustrated in Fig. S2c. Between charge transitions, the quantum dot acts like a floating island that does not screen the gate potential at all ($dV_{dot}/dV_g > 0$). At the charge transition, the quantum dot compensates by *overscreening* the gate potential giving a sudden drop in the dot potential ($dV_{dot}/dV_g < 0$). Over many charge transitions, the net effect is that the average dot potential stays fixed [6], as is the case for full screening

by a metal conductor ($dV_{dot}/dV_g = 0$). It is the overscreening at the negative steps in the dot potential that leads to the softening of the spring constant.

In Fig. 2C of the main text, we demonstrate that the frequency dip becomes broader and shallower with increasing bias across the dot. This can be understood from the effect of finite bias on the average dot occupation $\langle N(q_c) \rangle$: at large bias, the average occupation of the quantum dot changes more slowly as its chemical potential moves through the bias window. The derivative $d\langle N \rangle/dq_c$ is smaller, and hence the shift of the spring constant (Eq. S5) is also smaller. It is also interesting to note that for asymmetric tunnel barriers ($\Gamma_L \neq \Gamma_R$), the quantum dot occupation at higher bias changes more quickly at one edge of the Coulomb diamond, whereas the current does not. The peak in $d\langle N \rangle/dq_c$ therefore does not have to coincide with the maximum current of the Coulomb peak. This is also observed in the measurements, and can be seen clearly, for example, in Fig. S4.

S2.3 Coulomb blockade induced nonlinearity of the resonator

In section S2.2, we calculated the change in the linear spring constant of the mechanical resonator due to the force on the resonator from the Coulomb blockaded quantum dot. In addition to a correction to the linear coefficient, there will also be terms higher order in the displacement dz from Eq. S1. The Duffing parameter α , which determines the initial softening or hardening spring behaviour, can be calculated by taking the third derivative of the force d^3F/dz^3 . However, as we can read off $\Delta k(V_g)$ directly from the measured gate voltage dependence of the low-power resonance frequency, $f_0(V_g)$, we can also predict α from the experimental data:

$$\alpha = -\frac{d^3F}{dz^3} = \frac{d^2}{dz^2} \Delta k(q_c) = V_g^2 \left(\frac{dC}{dz} \right)^2 \frac{d^2(\Delta k)}{dq_c^2}, \quad (\text{S6})$$

again neglecting terms proportional to d^2C/dz^2 . The sign of α will follow the sign of the curvature of $\Delta k(V_g)$, as determined from the observed $f_0(V_g)$. This gives a change in the sign of α at the inflection points of the frequency dip, as illustrated in figure S3.

From the mechanical deformation of a beam under tension, we would normally expect a hardening spring behavior, as observed in previous nanotube experiments [3]. (This can also be seen from the overall positive curvature of the mechanical tuning of the resonance, shown in Fig. 1D of the main text.) The fact that we observe both softening and hardening behaviour with a small change in gate voltage indicates that the nonlinear coefficient from the single electron force, α_e , is much larger in magnitude than that from the mechanical deformation, α_{mech} : $|\alpha_e| \gg |\alpha_{mech}|$. Essentially, the single electron force dominates the nonlinearity of the resonator.

S2.4 Non-linear behaviour at high driving powers

Fig. S4 shows the data from Fig. 3 of the main text in both upwards and downwards frequency sweep directions, and as well for a power of -32.5 dB. The resonance at the highest powers displays a highly structured lineshape, particularly around the frequency dip, as can be seen in the waterfall plot (Fig. S5) of the -20 dB data.

S2.5 Suppression of switch ridges at low tunnel rates

In figure 4 of the main text, we present a peculiar instability in the Coulomb diamonds of clean, suspended carbon nanotube quantum dots. This instability appeared as ridges of sharp positive and negative spikes in the differential conductance, visible also as a sudden jump in the current. Unlike electronic excited states [7] or phonon sidebands [8, 9, 10, 11], the ridges of spikes do not run parallel to the Coulomb diamond edges, nor are they broadened by temperature or tunneling rates as the electronic excited states are: they often occur over just one pixel in the measurement. The spikes arise from a positive feedback mechanism between single electron tunneling and the mechanical motion that spontaneously drives the resonator into a high amplitude oscillation state [12]. The feedback mechanism in [12] requires a mechanical resonator with a very high quality-factor, a quantum dot with energy dependent tunneling, and a tunneling rate of electrons through the dot that is much faster than the mechanical resonance frequency. Essentially, for each mechanical oscillation of the nanotube, many electrons should tunnel through the quantum dot.

In Fig. S6, we show that, experimentally, this instability can be suppressed by reducing the rate at which electrons tunnel through the dot. This data is from device 2, in which the barriers to the leads changed very rapidly as we reduced the number of holes in the quantum dot. Although we did not have RF coax for measuring the mechanical resonance frequency of this device, we estimate the resonance frequency to be on the order of 100 to 500 MHz from the length of the nanotube. At high tunneling rates, corresponding to $\Gamma \gg f_0$, Coulomb diamonds all display ridges of spikes in dI/dV . In Fig. S6D, the dot is very weakly coupled to the leads, with a tunnel rate of 500 MHz at $V_{sd} = 4$ mV. Γ is no longer much larger than f_0 , and the instability is suppressed.

S3 Supplementary Figures

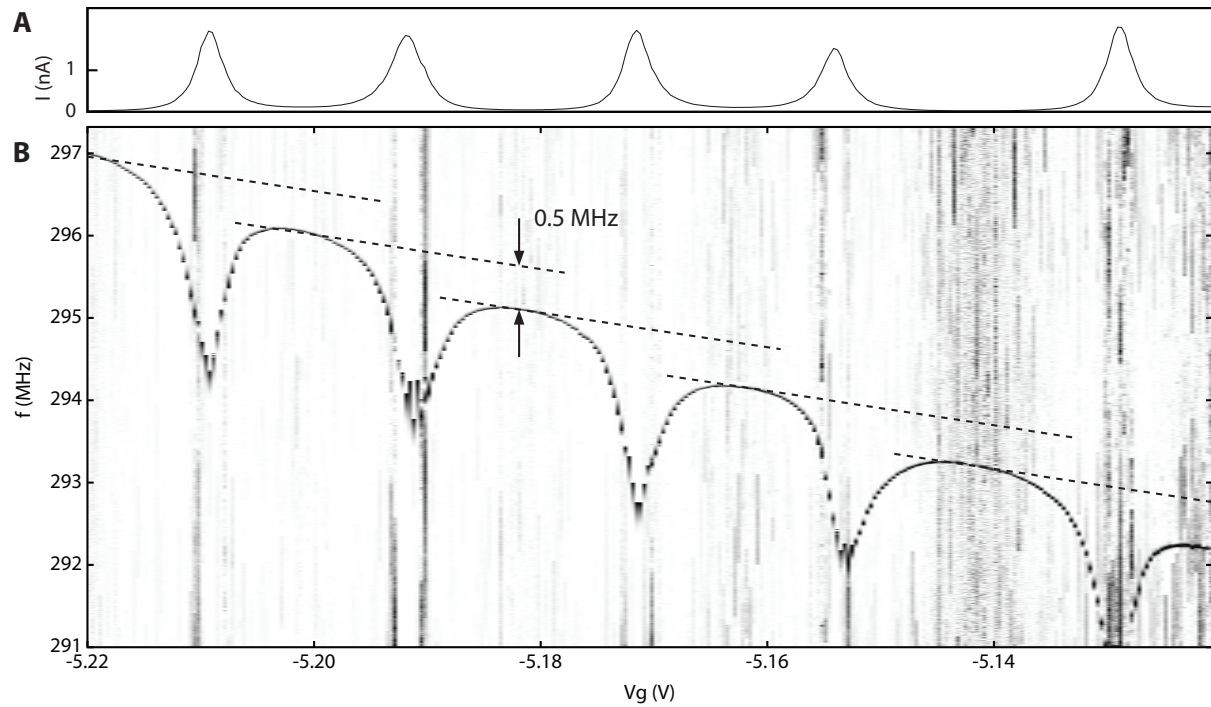


Fig. S1: (A) Coulomb peaks of the nanotube at $V_{sd} = 0.1$ mV and $V_g \sim -5$ V. (B) Normalized resonance signal $\Delta I / \Delta I_{peak}$, measured at an RF power of -38 dB. We observe shifts of the resonator frequency by 0.5 MHz due to the electrostatic force from a single electron.

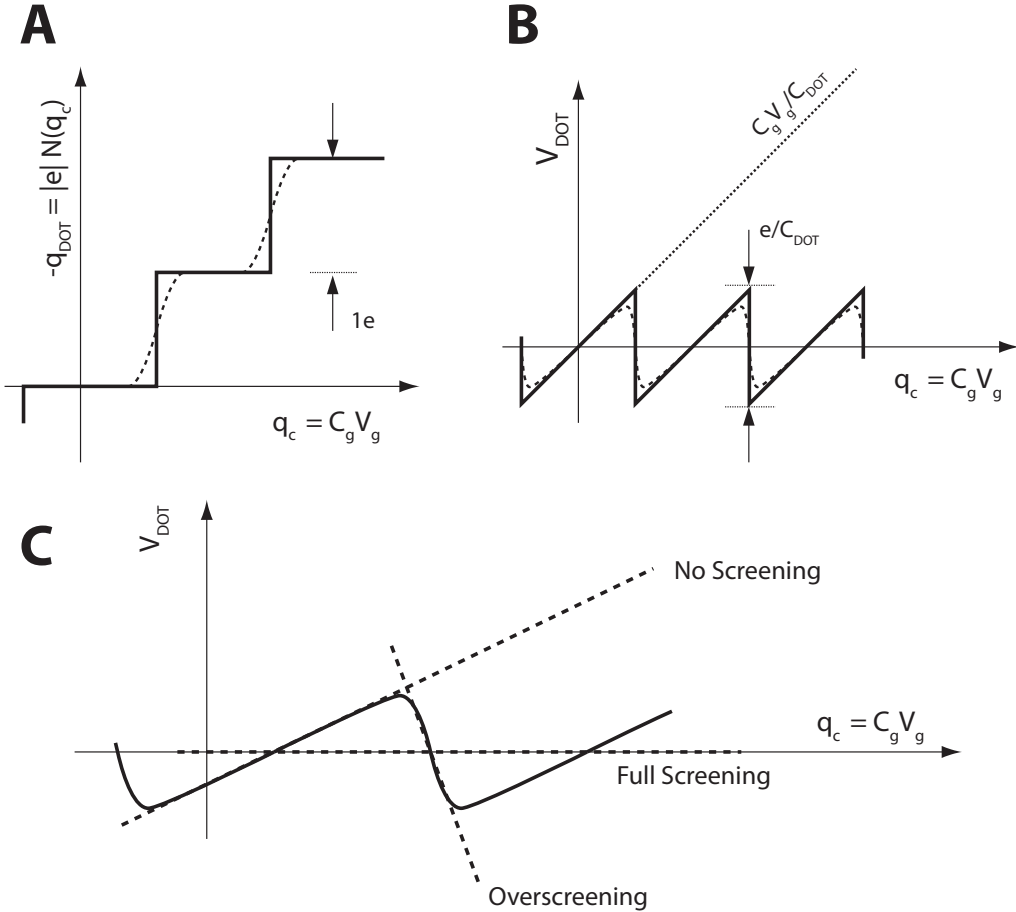


Fig. S2: (A) The charge on the quantum dot q_{dot} as a function of the control charge $q_c = C_g V_g$ follows a staircase with steps of e . The dashed line shows the average dot occupation $\langle N(q_c) \rangle$: the steps become broadened by charge fluctuations. (B) The potential of the quantum dot V_{dot} oscillates with a sawtooth waveform. On the rising edge, V_{dot} follows the potential of a floating conductor, $C_g V_g / C_{dot}$ (dotted line). Averaging over charge fluctuations, the sharp edges of the sawtooth become broadened ($\langle V_{dot} \rangle$ shown by dashed line). (C) shows the time averaged $\langle V_{dot} \rangle$ as a function of the control charge. Between charge transitions, the quantum dot charge is fixed, and does not screen V_g at all (no screening). At charge transitions, V_{dot} drops suddenly, overscreening V_g . On average, V_{dot} is constant (full screening).

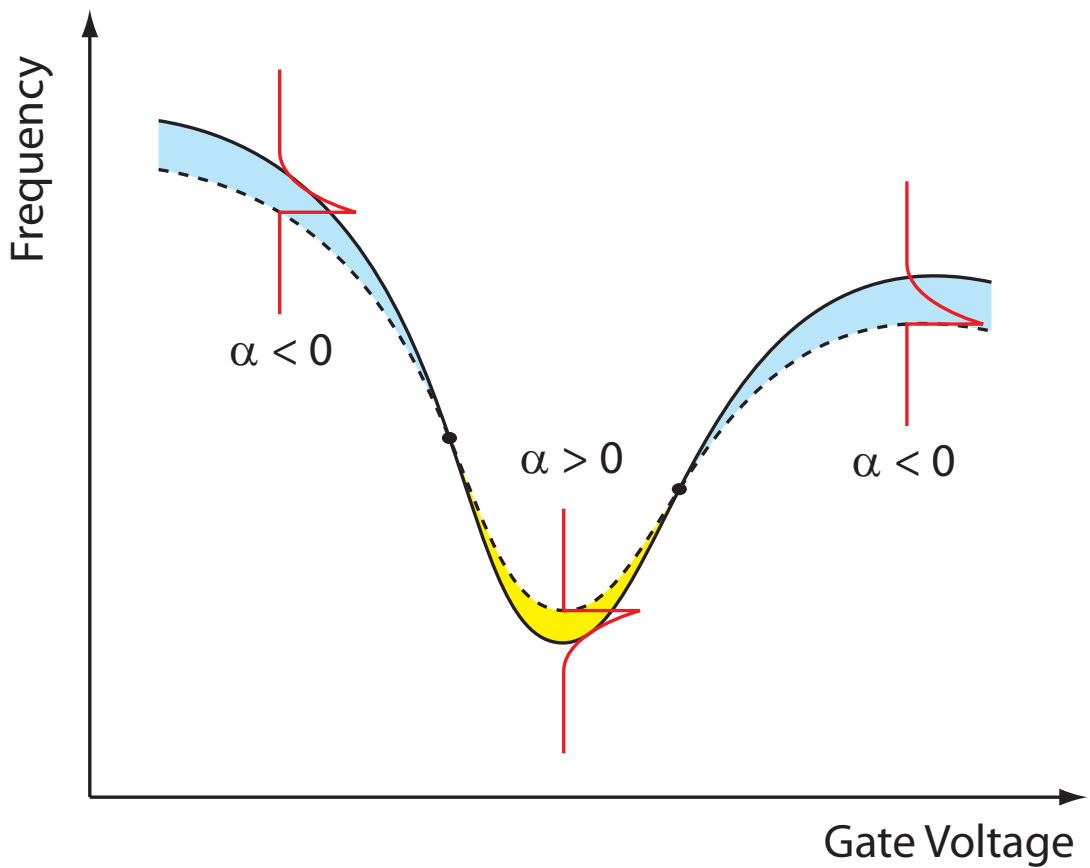


Fig. S3: The sign of the nonlinear Duffing parameter α is determined by the curvature of $f_0(V_g)$. The solid line shows the position of the resonance at low powers, f_0 . The dashed line shows the sharp edge of the non-linear resonance lineshape at higher powers (frequency traces illustrated by red lines). For positive curvature (yellow), we have $\alpha > 0$, and for negative curvature (blue), we have $\alpha < 0$.

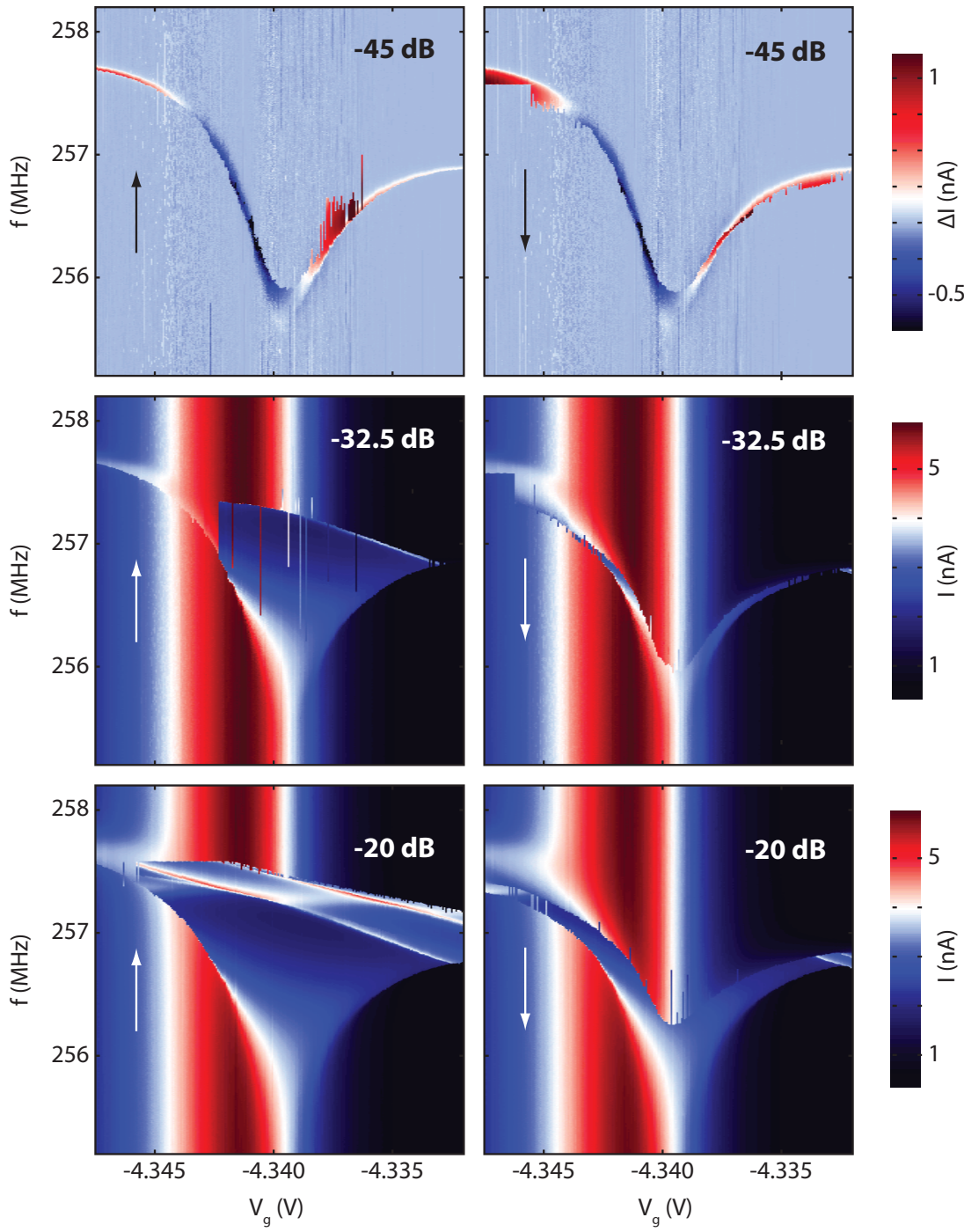


Fig. S4: Upwards (left column) and downwards (right column) frequency sweeps in the non-linear regime, taken at -45 dB, -32.5 dB and -20 dB for the same $V_{sd} = 0.5 \text{ mV}$ and V_g range as used in figure 3 of the main text. For the -45 dB data, the off-resonant current was subtracted from the data.

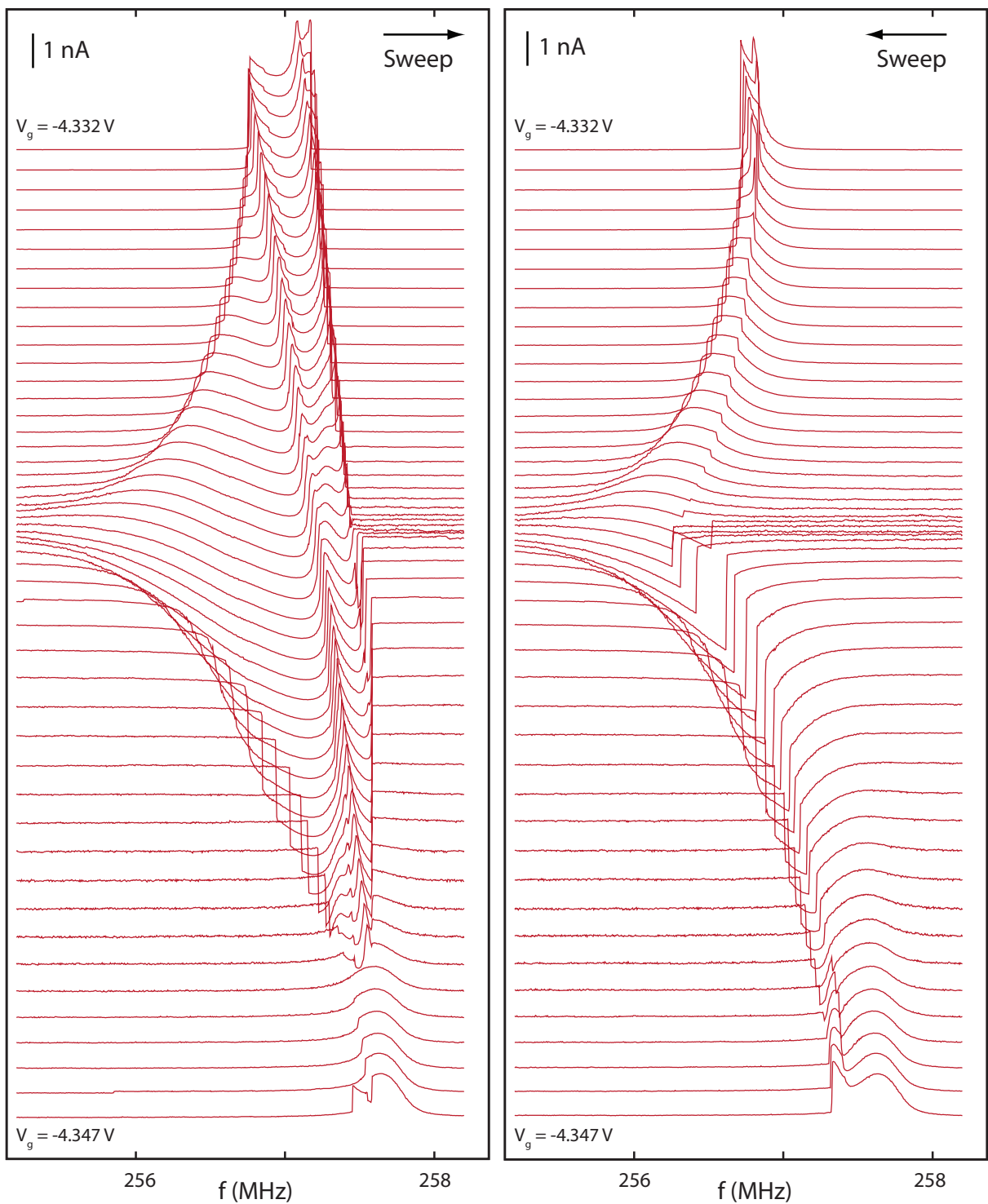


Fig. S5: A waterfall plot of upward (left) and downward (right) frequency sweeps at a power of -20 dB. Line cuts are data from the colorscale plots displayed in Fig. S4.

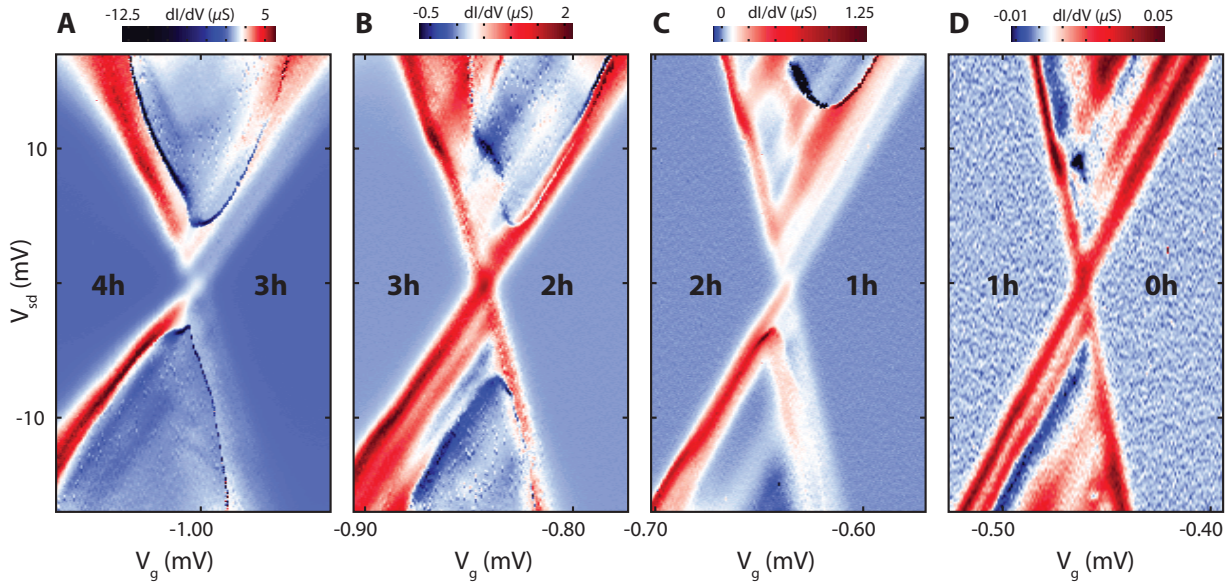


Fig. S6: Suppression of the mechanical instability by reducing tunnel rates using tunable barriers in device 2. (A) The data from figure 4(B) of the main text, showing spikes in the differential conductance dI/dV . (B) - (D) Reducing the number of holes in the quantum dot to zero, the tunnel barriers become more opaque. The spike ridges in the differential are initially pushed to higher bias, and then suppressed in the last Coulomb diamond. For a comparison, the current at a 4 mV bias in (A) - (D) is 7.3 nA, 3.1 nA, 0.5 nA, and 80 pA, corresponding to tunnel rates Γ of 45 GHz, 20 GHz, 3 GHz, and 500 MHz, respectively.

S4 Supplementary References

- [1] G. A. Steele, G. Gotz, L. P. Kouwenhoven, *Nature Nano.* **4**, 363 (2009).
- [2] A. K. Huettel, *et al.*, *Nano Letters* **9**, 2547 (2009).
- [3] V. Sazonova, *et al.*, *Nature* **431**, 284 (2004).
- [4] B. Witkamp, M. Poot, H. S. J. van der Zant, *Nano Lett.* **6**, 2904 (2006).
- [5] M. Brink, thesis, Cornell University (2007).
- [6] Here, we have neglected the energy level spacing in the quantum dot. Including it, the potential will on average increase with a small slope, but will still display negative steps that give the softening of the spring constant.
- [7] E. B. Foxman, *et al.*, *Phys. Rev. B* **47**, 10020 (1993).
- [8] H. Park, *et al.*, *Nature* **407**, 57 (2000).
- [9] S. Sapmaz, J. P. Herrero, Y. M. Blanter, C. Dekker, H. S. J. van der Zant, *Phys. Rev. Lett.* **96** (2006).
- [10] F. A. Zwanenburg, C. E. van Rijmenam, Y. Fang, C. M. Lieber, L. P. Kouwenhoven, *Nano Lett.* **9**, 1071 (2009).
- [11] R. Leturcq, *et al.*, *Nature Phys.* **5**, 327 (2009).
- [12] O. Usmani, Y. M. Blanter, Y. V. Nazarov, *Phys. Rev. B* **75**, 195312 (2007).